SUPPLEMENTARY INFORMATION

Observation of hidden atomic order at the interface between Fe and topological insulator Bi_2Te_3

Jaime Sánchez-Barriga, Ilya I. Ogorodnikov, Mikhail V. Kuznetsov, Andrey A. Volykhov, Fumihiko Matsui, Carolien Callaert, Joke Hadermann, Nikolay I. Verbitskiy, Roland J. Koch, Andrei Varykhalov, Oliver Rader and Lada V. Yashina

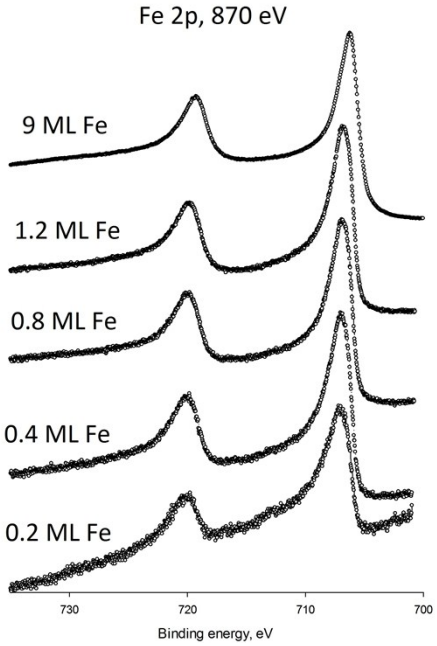

Fig. S1. Normalized Fe 2*p* core levels for different Fe coverages on Bi_2Te_3.

Table S1. Summary of the calculation results: Fermi level shifts and relative core level shifts for the different structure modeling of the Fe/Bi_2Te_3 interface (1 monolayer ML is calculated based on the bcc Fe crystal structure; as 1 atomic layer AL we assign the situation in which the amount of deposited Fe atoms is one to one Te atom in the first (upper) atomic layer of the clean surface, i.e. 1 AL=0.31 ML).

Structure	Coverage, AL	Coverage, ML	$-E_f$, eV	Relative energy of isomers, eV	Relative Te 4d shift, eV	Relative Bi 5d shift, eV	Fe coordi-nation
I –clean Bi_2Te_3 (111) surface	0	0	4.9784		0	0	
IIa -Bi_2Te_3 + Fe adatom in hollow position over Te in third layer (*fcc*H_3)	0.25	0.078	4.6307	+0.054	-0.0502	-0.1831	2 Bi, 1+3 Te
IIb - Bi_2Te_3 + Fe adatom in hollow position over Bi in second layer (*hcp*T4)	0.25	0.078	4.6679	0	-0.0914	-0.4514	1 Bi, 3 Te
IIc -Bi_2Te_3 + Fe atom in position of Bi, Bi at the surface over Fe	0.25	0.078	4.5521	+0.719	0.0175	-0.1913	1 Bi, 4 Te

IId- Bi_2Te_3 + Fe at the surface over Te	0.25	0.078	4.7889	+0.548	0.3587	-0.5287	6 Te
IIIa - Bi_2Te_3 + Fe adatom in hollow position over Te in third layer	0.5	0.155	4.7159	0	0.1791	-0.1876	2 Bi, 3 Te
IIIb - Bi_2Te_3 + Fe adatom in hollow position over Bi in second layer	0.5	0.155	4.6356	+0.589	0.0780	-0.4099	1 Bi, 3 Te
IV - Bi_2Te_3 + Fe adatom in hollow position over Te in third layer	0.75	0.233	4.8229		0.5715	-0.1059	3 Bi, 3 Te
Va - Bi_2Te_3 + Fe adatom in hollow position over Te in third layer	1	0.31	4.7864	0	0.3015	-0.259	3 Bi, 4 Te
Vb - Bi_2Te_3 + Fe adatom in hollow position over Bi in second layer	1	0.31	4.6189	+0.280	-0.4642	-0.2135	1 Bi, 3 Te
VIa - Bi_2Te_3 + Fe adatom in hollow position over Te in third layer, second Fe atom in hollow position over Bi in second layer	2	0.62	4.8185		0.6556	-0.2592	0-1 Bi, 3 Te
VIb - Bi_2Te_3 + Fe adatom in hollow position over Te in 3rd layer; interstitial Fe under Bi in 2nd layer	2	0.62	4.8176	+0.479	0.3867	-0.6717	3 Te; 1+3 Bi, 3 Te
VII - Bi_2Te_3 + Fe adatom in hollow position over Te in third layer, second atom is above Bi, third is above upper Te atom	3	0.93	4.4341		0.7594	-0.0466	1-3 Te
VIII	4	1.24	4.8611		0.3032	-0.1733	0-1 Te
IX	5	1.51	4.8013		0.6012	-0.0853	0-1 Te

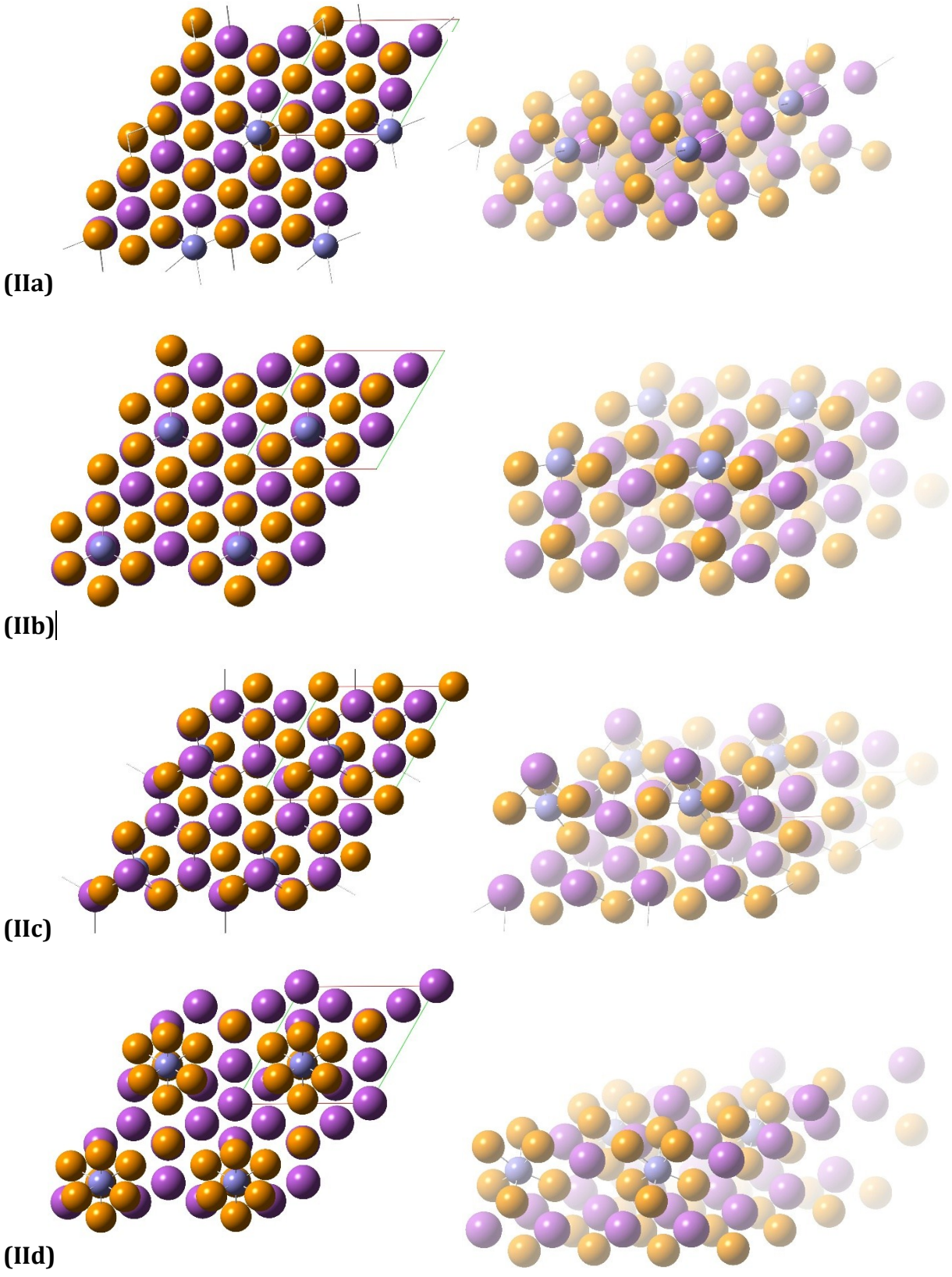

Fig. S2. Optimized structures modeling Fe-related point defects at the surface of Bi_2Te_3 (111). Bi, Te and Fe atoms are depicted in violet, orange, and blue color, respectively.

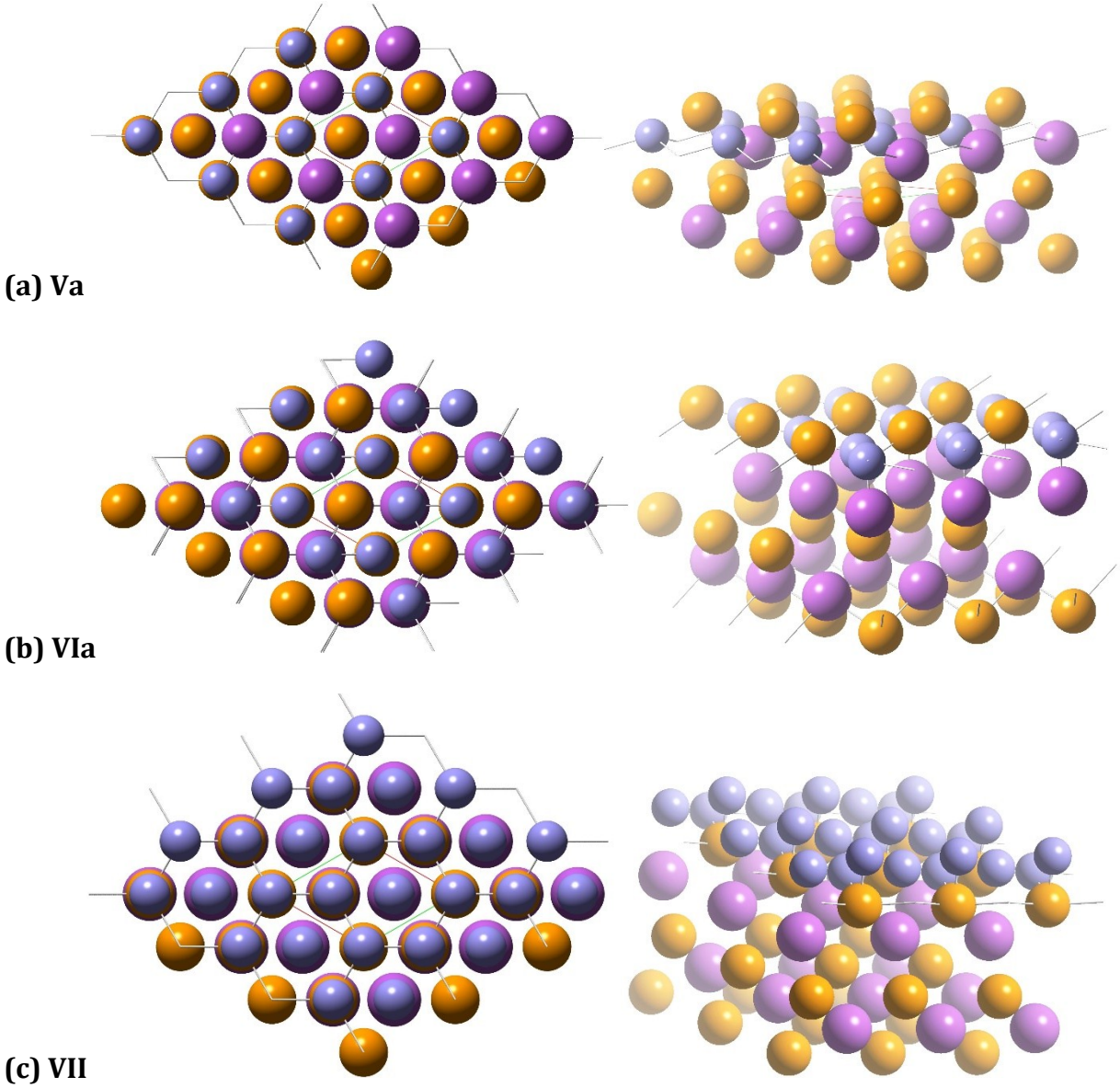

Fig. S3. The optimized geometry of the structures modeling adsorption of (a) 1, (b) 2 and (c) 3 atomic layers (ALs) of Fe on the Bi_2Te_3 (111) surface (1 AL=0.31 ML). Bi, Te and Fe atoms are depicted in violet, orange, and blue color, respectively. (a), (b) and (c) correspond to structures Va, VIa, VII in Table S1.

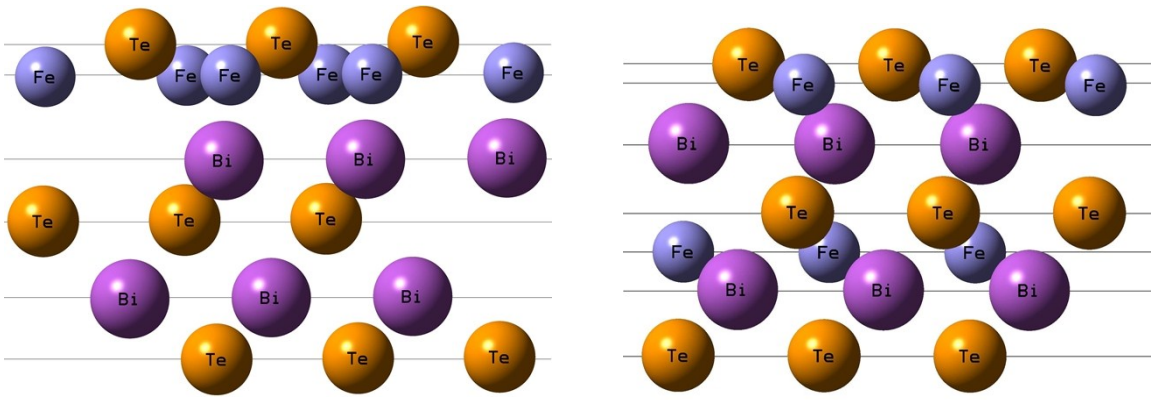

Fig. S4. Side view of the optimized geometry of the structures modeling adsorption of 2 atomic layers (ALs) of Fe on the Bi_2Te_3 (111) surface (1 AL=0.31 ML). Bi, Te and Fe atoms are depicted in violet, orange, and blue color, respectively.